MAGNETIC CONFINEMENT AND SCREENING MASSES

E.L.Gubankova[(a)] and Yu.A.Simonov[(b)]
(a)Institut für Theoretische Physik
Universität Heidelberg
Philosophenweg 19,D-69120 Heidelberg,FRG
(b)Institute of Theoretical and Experimental Physics
117259, Moscow, B.Cheremushkinskaya 25, Russia

Abstract

Confined and deconfined phases are defined through nonperturbative correlators and nonperturbative background perturbation theory is used to compute the critical temperature T_c and spatial string tension. Taking evolution along one of the spatial axes the set of Hamiltonians $H(n_1, n_2)$ with different Matsubara frequencies is obtained.

Meson and glueball screening masses and wave functions are computed for $H(0,0)$ and compared with available lattice data.

1. Finite temperature QCD, and in particular the dynamics of deconfinement phase transition and the physics beyond the critical temperature T_c is an important testing ground for our ideas about the nature of the QCD vacuum.

During the last few years, a lot of lattice data have appeared which point to the nonperturbative character of dynamics above T_c. To this belong i) the area law of spatial Wilson loops [1,2], ii)the screening masses of mesons and baryons [3-5] and glueballs [6], iii)the temperature dependence of Polyakov–line correlators [7-9]. In addition,the behavior of $\varepsilon - 3p$ above T_c has a bump incompatible with the simple quark–gluon gas picture [10]. Thus the inclusion of nonperturbative (NP) configurations into QCD at $T > 0$ and also at $T > T_c$ is necessary.

One of the authors has developed a systematic method for QCD, treating NP fields as a background and performing perturbative expansion around that both for $T = 0$ [11] and $T > 0$ [12].

To describe the phase transition, a simple choice of deconfined phase was suggested [12] where all NP color magnetic configurations are kept intact as in the confined phase, whereas color electric correlators that are responsible for confinement vanish.

This picture together with the background perturbation theory [11,12] forms a basis of quantitative calculations, where field correlators (condensates) are used as the NP input.

As an immediate check one computes T_c for a different number of flavours n_f in good agreement with lattice data. One purpose of the present letter is to treat quantitatively the points i)-iii) systematically in the framework of the same method. Doing so we meet some limitations. First, in the description of the deconfined phase in the spirit of the aforementioned method [12], one uses the magnetic correlators (and spatial string tension σ_s) from the lattice calculations [1,2]. In the confined phase below T_c and up to the temperatures $T \leq 1.5T_c$ in the

deconfined phase these correlators are practically the same as are known for $T = 0$. Therefore in the mentioned temperature region the spatial string tension σ_s is regarded as $T-$ independent and coincides with the standard string tension σ at $T = 0$. This is because the main dynamics (and contribution to the free energy) is due to the scale anomaly which essentially changes at the temperature of the order of the dilaton mass, i.e. at $T < 1GeV$. However, at large T, a new physics sets in: that of dimensional reduction, which causes σ_s to grow [2,13]. For temperatures larger than 1.5 T_c we have used the scaling behavior of $\sigma_s(T)$ from [2], that is consistent with the dimensional reduction regime. We confine ourselves to the region $0 \leq T < 2 \div 3T_c$ and consider problems i)-iii) point by point.

The second limitation is of technical character, since the proposed method is used for simplicity in conjunction with the $1/N_c$ expansion. Therefore values of T_c are computed in the leading and subleading orders of $1/N_c$ expansion and strictly speaking the conclusion obtained for the first order of deconfinement phase transition cannot be extended to $N_c = 2$.

To calculate the screening masses one should first write the Green function of quark–antiquark ($q\bar{q}$) or two gluons (gg) in terms of the Wilson loop average [14,15] and derive from it the Hamiltonian taking evolution along one of the spatial axes. In fact, one obtains a set of Hamiltonians, containing all higher Matsubara frequencies. Our results for mesons in general agree with one of the choices adopted before in [17], and justify in that special case the confining ansatz made there.

Of special importance are the gg Hamiltonian and the corresponding glueball screening masses (GSM). Here the lowest Matsubara frequency is zero and the next one is $2\pi T$. Therefore within our picture only the nonperturbative interaction between gluons – spatial string tension – determine the temperature behavior of the lowest GSM. In contrast to that, the meson screening masses for the lowest states have an additional temperature dependence through the lowest Matsubara frequency.

We calculate the GSM corresponding to lowest states and compare our results with recent lattice data [6]. With the scaling behavior $\sigma_s(T)$ [2] GSM forms the similar pattern to that of the meson case. This picture is in agreement with existing lattice data [7-9].

2. We derive here the basic formulas for the partition function, free energy and Green function in the nonperturbative background formalism at $T > 0$ [12]. The total gluonic field A_μ is split into a perturbative part a_μ and a nonperturbative background B_μ

$$A_\mu = B_\mu + a_\mu \tag{1}$$

where both B_μ and a_μ are subject to periodic boundary conditions. The principle of this separation is immaterial for our purposes here, and one can average over fields B_μ and a_μ independently using the 'tHooft's identity[1] (for more discussion see [18])

$$Z = \int DA_\mu exp(-S(A)) = \frac{\int DB_\mu \eta(B) \int Da_\mu exp(-S(B+a))}{\int DB_\mu \eta(B)} \tag{2}$$

$$\equiv << exp(-S(B+a) >_a >_B$$

with arbitrary weight $\eta(B)$. In our case we choose $\eta(B)$ to fix the field correlators and the string tension at their observed values. For simplicity have omitted gauge fixing and ghost terms in (2).

To the lowest order in ga_μ the partition function and free energy are

$$Z_0 =< exp(-F_0(B)/T) >_B,$$

[1] private communication to one of the authors (Yu.A.),December 1993.

$$F_0(B)/T=\frac{1}{2}lndetW-lndet(-D^2(B))=$$
$$=Sp\int^\infty_0\zeta(t)\frac{dt}{t}(-\frac{1}{2}e^{-tW}+e^{tD^2(B)}) \tag{3}$$

where $\hat{W}=-D^2(B)-2g\hat{F}$ and $D^2(B)$ is the inverse gluon and ghost propagator, respectively, $\zeta(t)$ is a regularizing factor [12].

The ghost propagator can be written as [11,12]

$$(-D^2)^{-1}_{xy}=<x|\int^\infty_0 dse^{sD^2(B)}|y>=\int^\infty_0 ds(Dz)^w_{xy}e^{-K}\Phi(x,y) \tag{4}$$

where standard notations [14,15] are used

$$K=\frac{1}{4}\int^s_0 d\lambda\dot{z}^2_\mu\ ,\quad \Phi(x,y)=Pexpig\int^x_y B_\mu dz_\mu$$

and a winding path integral is introduced [12]

$$(Dz)^w_{xy}=\lim_{N\to\infty}\prod^N_{m=1}\frac{d^4\zeta(m)}{(4\pi\varepsilon)^2}\sum^\infty_{n=0,\pm1,..}\int\frac{d^4p}{(2\pi)^4}e^{ip(\sum^\infty_{m=1}\ zeta(m)-(x-y)-n\beta\delta_{\mu4})} \tag{5}$$

with $\beta=1/T$. For the gluon propagator an analogous expression holds true, except that in (4) one should insert the gluon spin factor $P_F exp2g\hat{F}$ into $\Phi(x,y)$. For a quark propagator the sum over windings in (5) acquires a factor $(-1)^n$ and the quark spin factor is $expg\sigma_{\mu\nu}F_{\mu\nu}$ [12].

We are now in a position to make the expansion of Z and F in powers of ga_μ (i.e. perturbative expansion in α_s), and the leading–nonperturbative term Z_0,F_0 – can be represented as a sum of contributions with different N_c behavior of which we systematically will keep the leading terms $0(N^2_c),0(N_c)$ and $0(N^0_c)$.

To describe the temperature of deconfinement phase transition one should specify the phases and compute the associated free energy. For the confining phase to lowest order in α_s,the free energy is given by Eq.(3) plus contribution of the energy density ε at zero temperature

$$F(1)=\varepsilon V_3-\frac{\pi^2}{30}V_3T^4-T\sum_s\frac{V_3(2m_sT)^{3/2}}{8\pi^{3/2}}e^{-m_{s/T}}+0(1/N_c) \tag{6}$$

where ε is defined by the scale anomaly [18]

$$\varepsilon\simeq-\frac{11}{3}N_c\frac{\alpha_s}{32\pi}<(F^a_{\mu\nu}(B))^2> \tag{7}$$

and the next terms in (6) correspond to the contribution of mesons (we keep only pion gas) and glueballs. Note that $\varepsilon=0(N^2_c)$ while two other terms in (6) are $0(N^0_c)$.

For the high temperature or second phase we make an assumption that there all color magnetic field correlators are the same as in the first phase, while all color electric fields vanish. Since at $T=0$ color magnetic correlators (CMC) and color electric correlators (CEC) are equal due to the Euclidean 0(4) invariance, one has

$$<(F^a_{\mu\nu}(B))^2>=<(F^a_{\mu\nu})^2>_{el}+<(F^a_{\mu\nu})^2>_{magn};<F^2>_{magn}=<F^2>_{el} \tag{8}$$

The string tension σ which characterizes confinement is due to the electric fields [20,21], e.g. in the plane (i4)

$$\sigma=\sigma_E=\frac{g^2}{2}\int\int d^2x<E_i(x)\Phi(x,0)E_i(0)\Phi(0,x)>+... \tag{9}$$

where dots imply higher order terms in E_i.

The vanishing of σ_E implies that gluons and quarks are liberated,and this will contribute to the free energy in the deconfined phase via their closed loop terms (3),(4) with all possible windings. The CMC enter via the perimeter contribution $<\Phi(x,x)>\equiv\Omega$ (see (4)). As a result one has for the second high-temperature phase (cf.[12])

$$F(2)=\frac{1}{2}\varepsilon V_3-(N_c^2-1)V_3\frac{T^4\pi^2}{45}\Omega_g-\frac{7\pi^2}{180}N_cV_3T^4n_f\Omega_q+0(N_c^0) \tag{10}$$

where Ω_q and Ω_g are perimeter terms for quarks and gluons, respectively, the latter was estimated in [22] from the adjoint Polyakov line. In what follows we replace Ω by one for simplicity.

Comparing (6) and (10), and setting $F(1)=F(2)$ at $T=T_c$, one finds to order $0(N_c)$, disregarding all meson and glueball contributions

$$T_c=\left(\frac{\frac{11}{3}N_c\frac{\alpha_s<F^2>}{32\pi}}{\frac{2\pi^2}{45}(N_c^2-1)+\frac{7\pi^2}{90}N_cn_f}\right)^{1/4} \tag{11}$$

For the standard value of $G_2\equiv\frac{\alpha_s}{\pi}<F^2>=0.012GeV^4$ [19] (note that for $n_f=0$ one should use an approximately 3 times larger value of G_2 [19]) one has for $SU(3)$ and different values of $n_f=0,2,4$, respectively $T_c=$ 240, 150, 134. This should be compared with lattice data [10] $T_c(lattice)=240,146,131$.The agreement is quite good. Note that at large N_c, one has $T_c=0(N_c^0)$, i.e. the resulting value of T_c does not depend on N_c in this limit. Hadron contributions to T_c are $0(N_c^{-2})$ and therefore suppressed if T_c is below the Hagedorn temperature, as typically happens [23].

3. In this section we derive the area law for spatial Wilson loops, expressing spatial string tension in terms of CMC.

To this end we write $<W(C)>$ for any loop as [21]

$$<W(C)>=exp[-\frac{g^2}{2}\int d\sigma_{\mu\nu}(u)d\sigma_{\rho\lambda}(u')\ll F_{\mu\nu}(u)\Phi(u,u')F_{\rho\lambda}(u')\Phi(u',u)\gg \tag{12}$$

$$+\text{ higher order cumulants}]$$

For temporal Wilson loops, in the plane $i4, i=1,2,3$, only color electric fields $E_i=F_{i4}$ enter in (12), while for spatial ones in the plane $ik; i,k=1,2,3$ there appear color magnetic fields $B_i=\frac{1}{2}e_{ikl}F_{kl}$; in the standard way [21], one obtains the area law for large Wilson loops of size L, $L\gg T_g^{(m)}$ ($T_g^{(m)}$ is the magnetic correlation length)

$$<W(C)>_{spatial}\approx exp(-\sigma_sS_{\min}) \tag{13}$$

where the spatial string tension is [18]

$$\sigma_s=\frac{g^2}{2}\int d^2x\ll B_n(x)\Phi(x,0)B_n(0)\Phi(0,x)\gg+0(<B^4>) \tag{14}$$

and n is the component normal to the plane of the contour, while the last term in (14) denotes the contribution of the fourth and higher order cumulants. On general grounds, one can write for the integrand in (14)

$$\ll B_i(x)\Phi(x,0)B_j(0)\Phi(0,x)\gg=\delta_{ij}(D^B(x)+D_1^B(x)+\vec{x}^2\frac{\partial D_1^B}{\partial x^2})-x_ix_j\frac{\partial D_1^B}{\partial x^2}, \tag{15}$$

and only the term $D^B(x)$ enters in (14) [18]

$$\sigma_s = \frac{g^2}{2}\int d^2x D^B(x) + 0(< B^4 >) \tag{16}$$

This holds similarly for the temporal Wilson loop in the plane $i4$,so that one has the area law for $T < T_c$ with temporal string tension

$$\sigma_E = \frac{g^2}{2}\int d^2x D^E(x) + 0(< E^4 >) \tag{17}$$

For $T = 0$ due to the 0(4) invariance, CEC and CMC coincide and $\sigma_E = \sigma_s$. For $T > T_c$ in the phase (2) CEC vanish, while CMC change on the scale of the dilaton mass $\sim 1GeV$.Therefore one expects that σ_s stays intact till the onset of the dimensional reduction mechanism. This expectation is confirmed by the lattice simulation – σ_s stays constant up to $T \approx 1.4T_c$ [1,2]. Recent lattice data [2] show an increase of σ_s at $T \approx 2T_c$ for SU(2), which could imply the early onset of dimensional reduction.

4. In this section we consider the $q\bar{q}$ and gg Green functions $G(x, y)$ at $T > T_c$ and derive corresponding Hamiltonians for evolution in the spatial direction. We start with the Feynman–Schwinger representation [24] for $G(x, y)$, where for simplicity we neglect spin interaction terms

$$G(x, y) = \int_0^\infty ds \int_0^\infty d\bar{s} e^{-K-\bar{K}} (Dz)^w_{xy} (D\bar{z})^w_{xy} < W(C) > \tag{18}$$

Here K and $(Dz)^w_{xy}$ are defined in (5) and $< W(C) >$ in (12), where the contour C is formed by paths $z(\tau)$, $\bar{z}(\tau)$ and $t \equiv x - y$ is for definiteness taken along the 3'rd axis. Since by definition at $T > T_c$ electric correlators are zero, only elements $d\sigma_{\mu\nu}$ in (12) in planes 12,13 and 23 contribute. As a result one obtains for $< W(C) >$ the form (13) with

$$S_{min} = \int_0^t d\tau \int_0^1 d\gamma \sqrt{\dot{w}_i^2 w_k'^2 - (\dot{w}_i w_i')^2} \tag{19}$$

where only spatial components $w_i, i = 1, 2, 3$ enter

$$w_i(\tau, \gamma) = z_i(\tau)\gamma + \bar{z}_i(\tau)(1 - \gamma), \dot{w}_i = \frac{\partial w_i}{\partial \tau} \ , \quad w_i' = \frac{\partial w_i}{\partial \gamma} \tag{20}$$

The form (20) is equivalent to that used before in [14,15] but with $w_4 \equiv 0$.

As a next step one can introduce the "dynamical masses" $\mu, \bar{\mu}$ similarly to [14,15]. We are looking for the "c.m" Hamiltonian which corresponds to the hyperplane where $z_3 = \bar{z}_3$. Now the role of evolution parameter (time) is played by $z_3 = \bar{z}_3 = \tau$ with $0 \le \tau \le t$, and we define transverse vectors $z_\perp(z_1, z_2), \bar{z}_\perp(\bar{z}_1, \bar{z}_2)$ and $z_4(\tau), \bar{z}_4(\tau)$.

$$\frac{dz_3}{d\lambda} = \frac{d\tau}{d\lambda} = 2\mu, \quad \frac{d\bar{z}_3}{d\bar{\lambda}} = \frac{d\tau}{d\bar{\lambda}} = 2\bar{\mu} \tag{21}$$

Then $K, \bar{K}$ in (18) assumes the form

$$K = \frac{1}{2}\int_0^t d\tau [\frac{m_1^2}{\mu(\tau)} + \mu(\tau)(1 + \dot{z}_\perp^2 + \dot{z}_4^2)] \tag{22}$$

and the same for $\bar{K}$ with additional bars over $\mu, \dot{z}_\perp, \dot{z}_4$.

Performing the transformation in the functional integral (18) $dsDz_3(\tau) \to D\mu,\ \ d\bar{s}D\bar{z}_3(\tau) \to D\bar{\mu}$, one has

$$G(x,y) = \int D\mu D\bar{\mu} Dz_\perp D\bar{z}_\perp (Dz_4)^w_{xy} (D\bar{z}_4)^w_{xy} exp(-A) \tag{23}$$

with the action

$$A = K + \bar{K} + \sigma S_{min} \tag{24}$$

Note that $z_4, \bar{z}_4$ are not governed by NP dynamics and enter A only kinematically (through $K, \bar{K}$), and hence can be easily integrated out in (23) using Eq.(5) for the 4-th components – with $(x-y)_4 = 0$ (see [18] for more detail).

One can now proceed as was done in [15,16], i.e. one introduces auxiliary functions $\nu(\tau,\gamma), \eta(\tau,\gamma)$, defines center-of-mass and relative coordinates $\vec{R}_\perp, \vec{r}_\perp \equiv \vec{r}$, and finally integrates out $\vec{R}_\perp$ and $\eta(\tau,\gamma)$. The only difference from [15,16] is that now $z_4, \bar{z}_4$ do not participate in all those transformations. As a result one obtains

$$G(x,y) \sim \int D\nu D\mu D\bar{\mu} Dr e^{-A^{(1)}} \sum_{n,n_2} e^{-A_{n_1 n_2}} \tag{25}$$

here

$$A^{(1)}(\mu,\bar{\mu},\nu) = \frac{1}{2}\int_0^t d\tau [\frac{\vec{p}_r^2 + m_1^2}{\mu} + \frac{\vec{p}_r^2 + m_2^2}{\bar{\mu}} + \mu + \bar{\mu} + \sigma^2 r^2 \int_0^1 \frac{d\gamma}{\nu} + \int_0^1 \nu d\gamma + \tag{26}$$

$$+ \frac{\vec{L}^2/r^2}{\mu(1-\zeta)^2 + \bar{\mu}\zeta^2 + \int_0^1 d\gamma(\gamma-\zeta)^2\nu}]$$

$$A_{n_1 n_2} = \frac{1}{2}(\pi T)^2 \int_0^t d\tau (\frac{b^2(n_1)}{\mu(\tau)} + \frac{b^2(n_2)}{\bar{\mu}(\tau)}), \tag{27}$$

$b(n) = 2n$ for bosons and $2n+1$ for quarks. We also have introduced the radial momentum $\vec{p}_r$,the angular momentum $\vec{L}$

$$\vec{p}_r^2 \equiv \frac{(\vec{p}\vec{r})^2}{r^2} = (\frac{\mu\bar{\mu}}{\mu+\bar{\mu}})^2 \frac{(\vec{r}\dot{\vec{r}})^2}{r^2}, \quad \vec{L} = \vec{r} \times \vec{p} \tag{28}$$

and

$$\zeta(\tau) = \frac{\mu(\tau) + <\gamma> \int \nu d\gamma}{\mu + \bar{\mu} + \int \nu d\gamma}, \quad <\gamma> \equiv \frac{\int \gamma\nu d\gamma}{\int \nu d\gamma} \tag{29}$$

Let us define the Hamiltonian H for the given action $A = A^{(1)} + A_{n_1 n_2}$ in (25), integrating over $D\nu, D\mu, D\bar{\mu}$ around the extremum of A (this is an exact procedure in the limit $t \to \infty$). For the extremal values of the auxiliary fields, one has

$$\frac{\vec{p}^2 + m_1^2 + (b(n_1)\pi T)^2}{\mu^2(\tau)} = 1 - \frac{l(l+1)}{\vec{r}^2}(\frac{(1-\zeta)^2}{a_3^2} - \frac{1}{\mu^2})$$

$$\frac{\vec{p}^2 + m_2^2 + (b(n_2)\pi T)^2}{\bar{\mu}^2(\tau)} = 1 - \frac{l(l+1)}{\vec{r}^2}(\frac{\zeta^2}{a_3^2} - \frac{1}{\bar{\mu}^2}) \tag{30}$$

$$\frac{\sigma^2}{\nu^2(\tau,\gamma)}\vec{r}^2 = 1 - \frac{l(l+1)}{\vec{r}^2}\frac{(\gamma-\zeta)^2}{a_3^2}$$

where $a_3 = \mu(1-\zeta)^2 + \bar{\mu}\zeta^2 + \int d\gamma(\gamma-\zeta)^2\nu$ and ζ is defined by eq.(29).

After the substitution of these extremal values into the path integral Hamiltonian

$$G(x,y) = < x| \sum_{n_1 n_2} e^{-H_{n_1 n_2} t} |y > \tag{31}$$

one has to construct (performing proper Weil ordering [28]) the operator Hamiltonian acting on the wave functions.

Consider for simplicity the case $\vec{L}=0$.Then from (30), one obtains

$$H_{n_1n_2}=\sqrt{\vec{p}^2+m_1^2+(b(n_1)\pi T)^2}+\sqrt{\vec{p}^2+m_2^2+(b(n_2)\pi T)^2}+\sigma r \tag{32}$$

Here $\vec{p}=\frac{1}{i}\frac{\partial}{\partial\vec{r}}$ and $\vec{r}=\vec{r}_\perp$ is a $2d$ vector, $\vec{r}=(r_1,r_2)$; m_1,m_2 – current masses of quark and antiquark and $\sigma=\sigma_s$, for the gg system $m_1=m_2=0$ and $\sigma=\sigma_{adj}=\frac{9}{4}\sigma_s$for SU(3) [25].

Eigenvalues and eigenfunctions of $H_{n_1n_2}$

$$H_{n_1n_2}\varphi(r)=M(n_1,n_2)\varphi(r) \tag{33}$$

define the so–called screening masses and corresponding wave–functions, which have been measured in lattice calculations [3-6].

The lowest mass sector for mesons is given by H_{00}, where for $n_1=n_2=0$ one has $b(n_1)=b(n_2)=1$ in (32). For light quarks one can put $m_1=m_2=0$ and expand at large T square roots in (32) to obtain

$$H_{00}\approx 2\pi T+\frac{\vec{p}^2}{\pi T}+\sigma_s r,\quad M_{00}\approx 2\pi T+\varepsilon(T) \tag{34}$$

where $\varepsilon(T)=\frac{\sigma_s(T)^{2/3}}{(\pi T)^{1/3}}a$ and $a\simeq 1.74$ is the eigenvalue of the 2-D dimensionless Schrödinger equation.

Assuming the parametrization $\sqrt{\sigma_s}=cg^2(T)T$ with c being numerical constant different for $SU(2)$ and $SU(3)$ [2] and the scaling behavior of $g^2(T)$, one has $M_{00}\approx 2\pi T+O((\ln(T/\Lambda_T))^{-4/3}T)$ tending to twice the lowest Matsubara frequency,as was suggested before in [26].(This limit corresponds to the free quarks,propagating perturbativly in the space–time with the imposed antiperiodic boundary conditions along the 4th axis). Eq. (34) coincides with that proposed in [17],where also numerical study was done of M_{00} and $\varphi_{00}(r)$.Our calculations of Eq.(33-34) for $SU(3)$ with $c=0.586$ [2] agree with [17] and are presented in Fig.1 together with lattice calculations of $\varphi(r)_{00}$ for ρ–meson [5]. The values of $M_{00}(T)$ found on the lattice [3,4] are compared with our results in Fig.2. Note, that our M_{00} (34) does not contain perimeter corrections which are significant. Therefore one has to add the meson constant to M_{00} to compare with lattice data. We disregard the spin–dependent and one-gluon-exchange (OGE) interaction here for lack of space and will treat this subject elsewhere [18]. It is known [17], however, that OGE is not very important at around $T\approx 2T_C$.

We note that the lowest meson screening mass appears also in Yukawa type exchanges between quark lines and can be compared with the corresponding masses in Yukawa potentials.

5. For the gg system, the lowest mass sector is given by $b(n=0)=0$, and one has from (32)

$$H_{00}(gg)=2|\vec{p}|+\sigma_{adj}r \tag{35}$$

Note that T does not enter the kinetic terms of (35).

To calculate with (35) one can use the approximation in (26) of τ–independent μ [14], which leads to the operator ($\mu=\bar{\mu}$)

$$h(\mu)=\mu+\frac{\vec{p}^2}{\mu}+\sigma_{adj}r \tag{36}$$

The eigenvalue $E(\mu)$ of $h(\mu)$ should be minimized with respect to μ and the result $E(\mu_0)$ is known to yield the eigenvalue of (35) within a few percent accuracy [27]. The values $E(\mu_0)\approx M_{gg}$ thus found are presented in Fig.2. The corresponding wave functions $\varphi_{00}(r)$ are given in

Fig.1. These data can be compared with the glueball screening masses, found on the lattice in [6].

Another point of comparison is the Polyakov line correlator

$$P(R)=\frac{<\Omega^+(R)\Omega(0)>}{<\Omega^+(R)><\Omega(0)>}=exp(-V(R)/T) \tag{37}$$

with

$$V(R)=\frac{exp(-MR)}{R^\alpha}\ ,\quad \Omega(R)=\frac{1}{N_C}trPexp(ig\int_0^\beta A_4dz_4)$$

It is easy to understand that $M=M_{gg}$ and one can compare our results for the GSM $M_{gg}(T)$ with the corresponding lattice data for M in Fig.2.

Taking again into account an unknown constant perimeter correction to our values of M_{gg}, one can see a reasonable qualitative behavior. We refer the reader to another publication for more detail [18].

In addition to the purely nonperturbative source of GSM described above there is a competing mechanism – the perturbative formation of the electric Debye screening mass $m_{el}(T)=gT(\frac{N_c}{3}+\frac{n_f}{6})$ for each gluon with $g(T)$ given by the temperature dependence of $\sqrt{\sigma_s(T)}=cg^2(T)T$ [2]. Therefore for large T, where m_{el} is essential, one should rather use instead of (35) another Hamiltonian, which is obtained from (32) replacing $m_1=m_2=m_{el}(T)$

$$\tilde{H}_{00}(gg)=2\sqrt{\vec{p}^2+m^2_{el}(T)}+\sigma_{adj}(T)r \tag{38}$$

It turns out that up to temperatures $T\leq 2T_c$, one can consider the effect of $m_{el}(T)$ as a small correction to the eigenvalue of (35) E

$$M_{gg}=E+\delta E\approx 4(\frac{a}{3})^{3/4}\cdot\frac{3}{2}cg^2(T)T+\frac{T}{\frac{3}{2}c(\frac{a}{3})^{3/4}} \tag{39}$$

where $a\simeq 1.74$ and this justifies our nonperturbative treatment of the GSM in the temperature region concerned.

We note that the transition between these two regimes (with the dominance of nonperturbative and then perturbative dynamics) is smooth, with the GSM tending to twice the Debye mass at large T [18].

6. In conclusion, we have pursued a selfconsistent analysis of nonperturbative dynamics at $T>T_c$, including the calculation of T_c, spatial area law and meson and glueball screening masses. We stress that in both meson and glueball cases, the nonperturbative mechanism plays an essential role in the formation of the screening masses in the temperature region $0<T<2\div 3T_c$, while at large T, the lowest screening masses tend to the corresponding limits, governed by perturbative dynamics. We obtain in all cases a reasonable agreement with known lattice data supporting our picture of magnetic confinement above T_c, while there is electric confinement below T_c. An additional piece of data is necessary to confirm our picture, e.g. lattice calculation of the screening glueball wave function to compare with our prediction.

One of us (E.G.) is grateful to B.L. Ioffe and V. Eletskii for useful discussions. The authors are grateful to D. Melikhov for help in computations. This work was supported by the Russian Fund for Fundamental Research, grant 93-02-14937.

References

[1] E.Manousakis and J.Polonyi, Phys. Rev. Lett. **58** (1987) 847;
C.Borgs,Nucl.Phys.**B 261**(1985)455

[2] G.S.Bali et al. Phys. Rev. Lett **71** (1993) 3059;
F.Karsch et al.Phys.Lett. **B346**(1995)94

[3] C.De Tar, Phys. Rev. **D 32** (1985) 276; ibid **D37** (1987) 2328

[4] C.De Tar and J.Kogut, Phys. Rev. Lett. **59** (1987) 399; Phys. Rev. **D36** (1987) 2828

[5] C.Bernard et al., Phys.Rev. Lett. **68**(1992) 2125

[6] B.Grossmann et al. Nucl. Phys. B417 (1994) 289

[7] S.Gottlieb et al. Nucl. Phys. B (Proc. Suppl.) **26** (19920 308

[8] M.Gao, Nucl. Phys. B (Proc. Suppl.) **9** (1989) 368

[9] P.Lacock and T.Reisz, Nucl. Phys. B (Proc. Suppl.) **30** (1993) 30

[10] F.Karsch in: "QCD: 20 years later"

[11] Yu.A.Simonov, HD-THEP-93-16, hep-ph 9311247, Yad. Fiz. (in press), JEPT Lett. **57** (1993) 513

[12] Yu.A.Simonov, hep-ph 9311216, Yad. Fiz. (in press), JEPT Lett. **55** (1992) 605

[13] S.Nadkarni, Phys.Rev. **D27** (1983) 917;
B.Petersson and T.Reisz, Nucl. Phys. **B353** (1991) 757

[14] Yu.A.Simonov, Phys.Lett. **226** (1989) 151

[15] A.Yu.Dubin, A.B.Kaidalov and Yu.A.Simonov, Phys.Lett. **B323** (1994) 41

[16] E.L.Gubankova, A.Yu.Dubin, Preprint ITEP 62-94; HEP-PH 9408278

[17] V.Koch, E.V.Shuryak, G.E.Born and A.D.Jackson, Phys.Rev. **D46** (1992) 3169

[18] E.L.Gubankova and Yu.A.Simonov (in preparation).

[19] M.A.Shifman, A.I.Vainshtein and V.I.Zakharov, Nucl. Phys. **B147** (1979) 385, 448

[20] H.G.Dosch, Phys. Lett. **190** (1987) 177.

[21] H.G.Dosch and Yu.A.Simonov, Phys. Lett. **B205** (1988) 339.

[22] H.G.Dosch, H.J.Pirner and Yu.A.Simonov (in preparation)

[23] J.Polehinski, et al. Phys. Rev. Lett. **68** (1992) 1267; Phys.Rev **46**(1992) 3667.

[24] Yu.A.Simonov, Nucl. Phys. **B 307** (1988) 512;
Yu.A.Simonov and J.A.Tjon, Ann. Phys, **228** (1993) 1

[25] I.J.Ford et al., Phys. Lett. **B208** (1988) 286

[26] V.Eletskii and B.L.Ioffe, Yad. Fiz. **47** (1988) 380

[27] Yu.A.Simonov, Yad. Fiz. **54** (1991) 192

[28] T.D.Lee, Particle Physics and Introduction to Field Theory. Harwood Academic Publishers. Forth Edition 1990.

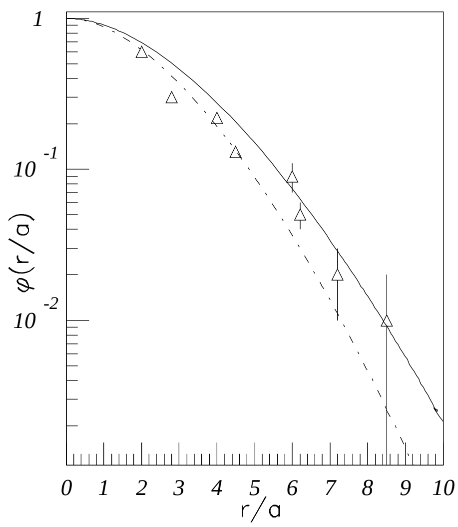

Figure 1: Wave functions for the ρ–meson (solid line) and glueball (dashed line) vs r/a (a=0.23 fm) for $T = 210$ MeV. The data from ref.[5] correspond to $T \approx 210$ MeV.

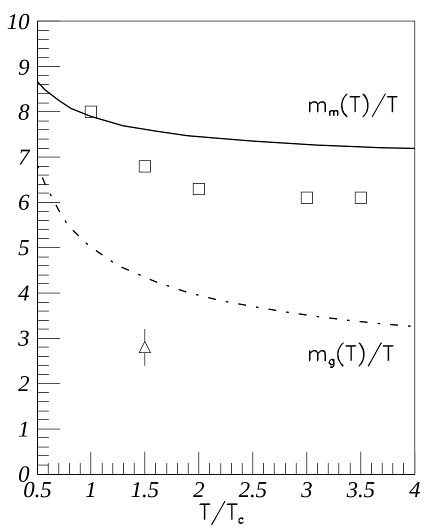

Figure 2: The screening masses for mesons (solid line) and glueballs (dashed line) as a function of temperature. The data from refs.[3,4] (squares) and [6] (triangle).